Problem Set 11
Physics 480 / Fall 1999
Professor Klaus Schulten

Solutions prepared by Sinan Arslan

Problem1: Scattering by a Spherical Potential Well

(a) The total cross section is defined through

$$\sigma_{tot} \;=\; 2\pi \int_0^\pi \sin\theta \, d\theta \frac{d\sigma}{d\Omega} \tag{1}$$

Inserting the expression for the differential cross section into (1) one obtains

$$\begin{aligned}\sigma_{tot} &= \frac{2\pi}{k^2} \int_0^\pi \sin\theta d\theta \sum_{\ell=0}^{\infty} (2\ell+1)\, e^{i\delta_\ell} \sin\delta_\ell \, P_\ell(\cos\theta) \sum_{\ell'=0}^{\infty} (2\ell'+1)\, e^{-i\delta_{\ell'}} \sin\delta_{\ell'} \, P_{\ell'}(\cos\theta) \\ &= \frac{2\pi}{k^2} \sum_{\ell=0}^{\infty} \sum_{\ell'=0}^{\infty} (2\ell+1)\,(2\ell'+1)\, e^{i\delta_\ell} \sin\delta_\ell \, e^{-i\delta_{\ell'}} \sin\delta_{\ell'} \int_0^\pi \sin\theta d\theta P_\ell(\cos\theta)\, P_{\ell'}(\cos\theta)\end{aligned} \tag{2}$$

By using the orthogonality relation of Legendre polynomials,

$$\int_0^\pi \sin\theta d\theta P_\ell(\cos\theta)\, P_{\ell'}(\cos\theta) \;=\; \frac{2}{2\ell+1} \delta_{\ell\ell'} \tag{3}$$

one arrive at the desired result

$$\sigma_{tot} \;=\; \frac{4\pi}{k^2} \sum_{\ell=0}^{\infty} (2\ell+1) \sin^2\delta_\ell \;. \tag{4}$$

(b) In classical mechanics, an incoming particle scattered by a spherical potential well is characterized by an impact parameter b. The angular momentum of the particle is conserved, and its magnitude is given by $L = p\,b = \hbar\,k\,b$, where $p = \hbar k$ is the linear momentum outside the potential well. Clearly, a particle with impact parameter $b > a$ will not be deflected. In quantum mechanics, both concepts of trajectory and impact parameter are meaningless. However, when the de Broglie wavelength of the particle is much smaller than the size of the potential well, i.e., $\lambda \sim 1/k \ll a$, or equivalently $ka \gg 1$, the particle behaves semi-classically. Hence, only partial waves corresponding to $L = \hbar\sqrt{\ell(\ell+1)} \approx \hbar \lesssim \hbar ka$ will contribute to σ_{tot}, i.e., in Eq. (4) $\ell \leq \ell_{max} = k\,a$.

(c) The radial wave function $v_\ell(r) = r\phi_{\ell,E}(r)$ can be found by solving the corresponding radial Schrödinger equation

$$\left[\frac{d^2}{dr^2} + \frac{2m}{\hbar^2}[E - U(r)] - \frac{\ell(\ell+1)}{r^2} \right] v_\ell(r) \;=\; 0 \;. \tag{5}$$

Outside the well $U(r > a) = 0$ and the solution to Eq. (5) can be written as a linear combination of the spherical Bessel and Neumann functions, i.e.,

$$v_\ell(r) \;=\; \beta_\ell \, j_\ell(kr) \,+\, \gamma_\ell \, n_\ell(kr) \;, \quad \text{for} \quad r > a \;, \tag{6}$$

where $k = \sqrt{2mE}/\hbar$. Inside the well $U(r < a) = -|U_o|$, and the radial wave function has a similar expression as above, except that this time the coefficient in front of the spherical Neumann function must be set equal to zero. This is because $n_\ell(r)$ diverges for $r \to 0$, and $v_\ell(r)$ must be finite at the origin. Hence,

$$v_\ell(r) \ = \ \alpha_\ell \, j_\ell(Kr) \ , \quad \text{for} \quad r < a \ , \tag{7}$$

where $K = \sqrt{2m(E - U_o)}/\hbar$.

(d) By matching the solutions (6) and (7), together with their derivatives, at $r = a$, one obtains

$$\gamma_\ell = \alpha_\ell \, \frac{k\, j_\ell(Ka) j_\ell^{'}(ka) - K\, j_\ell(ka) j_\ell^{'}(Ka)}{k\, n_\ell(ka) j_\ell^{'}(ka) - k\, j_\ell(ka) n_\ell^{'}(ka)} \tag{8}$$

and

$$\beta_\ell = -\alpha_\ell \, \frac{k\, j_\ell(Ka) n_\ell^{'}(ka) - K\, n_\ell(ka) j_\ell^{'}(Ka)}{k\, n_\ell(ka) j_\ell^{'}(ka) - k\, j_\ell(ka) n_\ell^{'}(ka)} \tag{9}$$

In terms of the phase shift δ_ℓ, the asymptotic behavior ($r \to \infty$) of the radial wave function is given by

$$\begin{aligned} v_\ell(k,\, r) \ &\sim \ \frac{\sin\left(kr \ - \ \frac{\ell\pi}{2} \ + \ \delta_\ell(k)\right)}{kr} \qquad (10) \\ &= \ \frac{\sin\left(kr \ - \ \frac{\ell\pi}{2}\right)}{kr} \cos\delta_\ell(k) + \frac{\cos\left(kr \ - \ \frac{\ell\pi}{2}\right)}{kr} \sin\delta_\ell(k) \ . \end{aligned}$$

By using the asymptotic form of the spherical Bessel functions

$$j_\ell(kr) \ \sim \ \frac{\sin\left(kr - \frac{l\pi}{2}\right)}{kr} \ , \quad \text{and} \quad n_\ell(kr) \ \sim \ -\frac{\cos(kr - \frac{l\pi}{2})}{kr} \ , \tag{11}$$

for large r, Eq. (6) becomes

$$v_\ell(k, r) \ \sim \ \frac{\sin\left(kr \ - \ \frac{\ell\pi}{2}\right)}{kr} \, \beta_\ell - \frac{\cos\left(kr \ - \ \frac{\ell\pi}{2}\right)}{kr} \, \gamma_\ell \ . \tag{12}$$

The phase shift can be determined by comparing Eqs. (10) and (12)

$$\tan\delta_\ell(k) \ = \ -\frac{\gamma_\ell}{\beta_\ell} = \frac{ka\, j_\ell(Ka) j_\ell^{'}(ka) - Ka\, j_\ell(ka) j_\ell^{'}(Ka)}{ka\, j_\ell(Ka) n_\ell^{'}(ka) - Ka\, n_\ell(ka) j_\ell^{'}(Ka)} \ . \tag{13}$$

The ℓ dependence of the phase shift δ_ℓ is shown in the left panel of Fig. 1.

(e) The differential cross section, as a function of θ, is plotted in the right panel of Fig. 1.

(f) The total cross section calculated with `Mathematica` is $\sigma_{tot} \ = \ 3.58\, a^2$ (slightly larger than the classical πa^2 value).

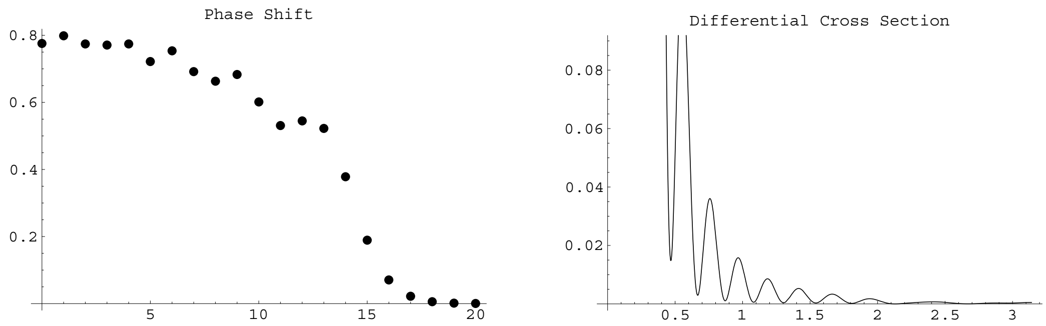

Fig. 1: δ_ℓ vs ℓ (left), and $d\sigma/d\Omega$ vs θ (right). Note that δ_ℓ decreases dramatically for $\ell \geq \ell_{max} = 16$.

Problem 2: Resonant Scattering States for a Spherical Potential Well

(a) For $\ell = 0$ the radial Schrödinger equation (5) becomes

$$\left(\frac{d^2}{dr^2} - \frac{2m}{\hbar^2}[|E| + U(r)]\right) v(r) = 0 \,, \tag{14}$$

where, for bound states, $E < 0$. Keeping in mind that the radial wave function must vanish for $r \to \infty$, and be finite for $r = 0$, the solution to Eq. (14) has the form

$$v_\ell(r) \;=\; \begin{cases} A\,\frac{\sin Kr}{r} & r \,<\, a \\ B\,\frac{e^{-\alpha r}}{r} & r \,>\, a \end{cases} \,, \tag{15}$$

where $\alpha = \sqrt{2m|E|}/\hbar$ and $K = \sqrt{2m(U_o - |E|)}/\hbar^2$. From the continuity of the logarithmic derivative of $v(r)$ at $r = a$ one obtains the following transcendental equation

$$K \cot Ka \;=\; -\alpha \;=\; -\sqrt{\frac{2mU_o}{\hbar^2} - K^2} \,, \tag{16}$$

whose solutions determine the energies of the bound states with $\ell = 0$. Equation (16) is equivalent to

$$\sin\, Ka \;=\; \pm\, Ka\sqrt{\hbar^2/2ma^2U_o} \,, \tag{17}$$

which can be solved graphically. By using the substitution $x = Ka$, Eq. (16) becomes

$$|\sin\, x| \;=\; (\sqrt{\hbar^2/2ma^2U_o})\, x \,. \tag{18}$$

The solution to this equation are given by the intersections of $|\sin\, x|$ with a line which passes through the origin, and has a slope proportional to $1/\sqrt{U_o}$ (see Fig. 2). From Eq. (17), it is clear that $\cot\, x \,<\, 0$, which means that $(2m + 1)\pi/2 \leq x \leq (2m + 1)\pi$ must hold, with $k \in \mathbb{N}$ (see the highlighted parts on the plot of $|\sin\, x|$ in Fig. 2). Now a simple inspection of Fig. 2 tells us that the minimum value of U_o for which the well can accommodate one bound state is determined by the condition $x = \pi/2$. Indeed, as we increase U_o (from zero) the slope of the line in

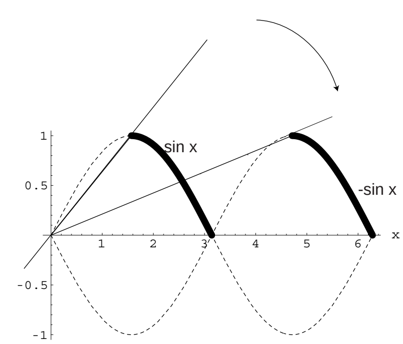

Fig. 2: Graphical solution of Eq. (17).

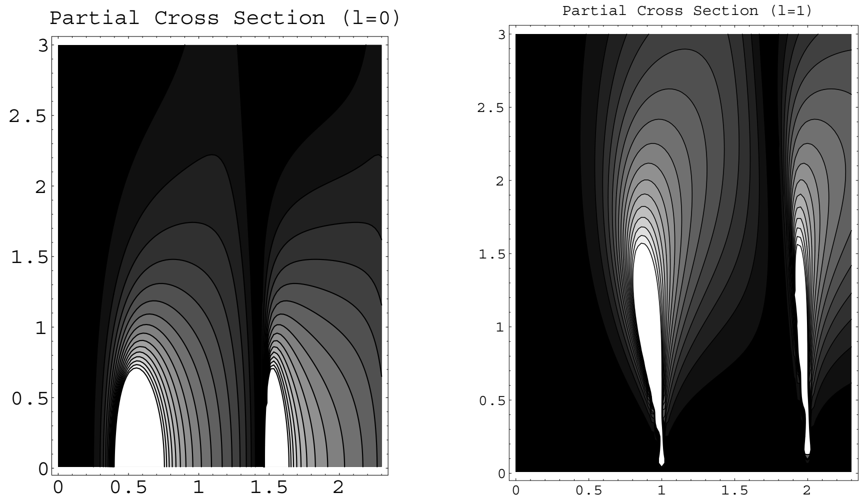

Fig. 3: Contour plots of σ_ℓ vs $\sqrt{U_o}$ (horizontal axis) and k (vertical axis) for $\ell = 0$ (left) and $\ell = 1$ (right).

Fig. 2 decreases and intersects for the first time the relevant (highlighted) parts of the $|\sin x|$ curve exactly at $x = Ka = \pi/2$. Hence,

$$U_o^{min} = \left(\frac{\pi}{2}\right)^2 \frac{\hbar^2}{2ma^2} = \frac{\pi^2\hbar^2}{8ma^2} \,. \tag{19}$$

Following the same strategy, one can easily see that the minimum value of U_o for which one has $m \in \mathbb{N}^*$ bound states in the well is given by

$$U_o^{(m)} = \left[(2m+1)\frac{\pi}{2}\right]^2 \frac{\hbar^2}{2ma^2} = (2m+1)^2 \frac{\pi^2\hbar^2}{8ma^2} \,. \tag{20}$$

(b) In the new units

$$\sigma_t = \sum_{l=0}^{\infty} \sigma_\ell = \frac{4\pi}{k^2} \sum_{\ell=0}^{\infty} (2\ell+1) \sin^2 \delta_\ell \tag{21}$$

where $\tan \delta_\ell$ is given by Eq. (13), with $a = 1$ and $K = \sqrt{k^2 + \pi^2 U_o}$.

(c) `ContourPlots` of $\sigma_\ell(k, \sqrt{U_o})$ in Fig. 3 and Fig. 4, are produced with `Mathematica` for $\ell = 0, 1, 2, 3$.

(d) The total cross section can be obtained by adding up σ_ℓ's up to $\ell_{max} = 4k$. The result is shown in Fig. 5.
(e) According to Fig. 5, the first three lowest order resonances occur for the following (approximate) values of ($\sqrt{U_o}$,k): **A** (0.5 , 0.1), **B** (0.98 , 0.35) and **C** (1.41 , 0.573). A comparison of Figs. 3, 4 and 5. suggests that the resonance islands in σ_t originates mainly from a single, similar resonance in one particular partial scattering cross section σ_ℓ. This does not come as a surprise if one realizes that a resonant state can also be regarded as a *pseudo bound state* in the effective potential

$$V_{eff} = V(r) + \frac{\hbar^2 \ell(\ell+1)}{2mr^2} \tag{22}$$

In Fig. 6 σ_ℓ vs ℓ is plotted for the above identified ($\sqrt{U_o}$,k) values.
(f) The radial wave functions for the resonant states A, B, and C are plotted in Fig. 7

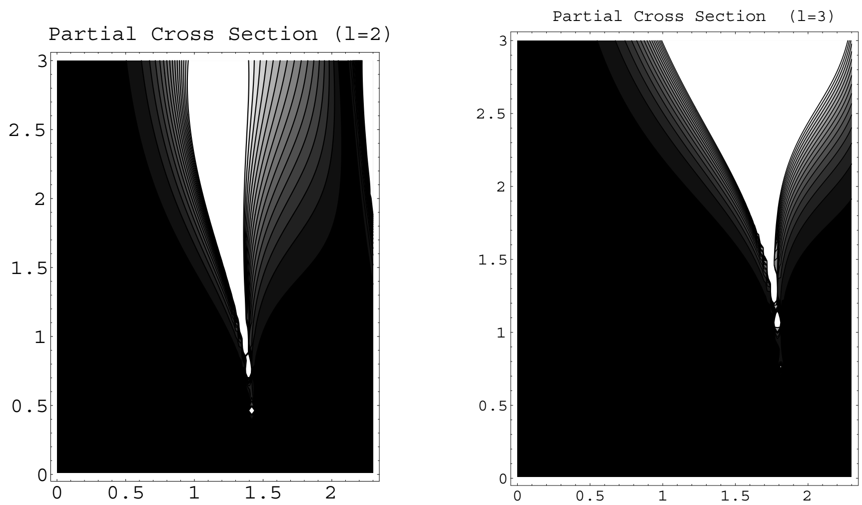

Fig. 4: Contour plots of σ_ℓ vs $\sqrt{U_o}$ (horizontal axis) and k (vertical axis) for $\ell = 2$ (left) and $\ell = 3$ (right).

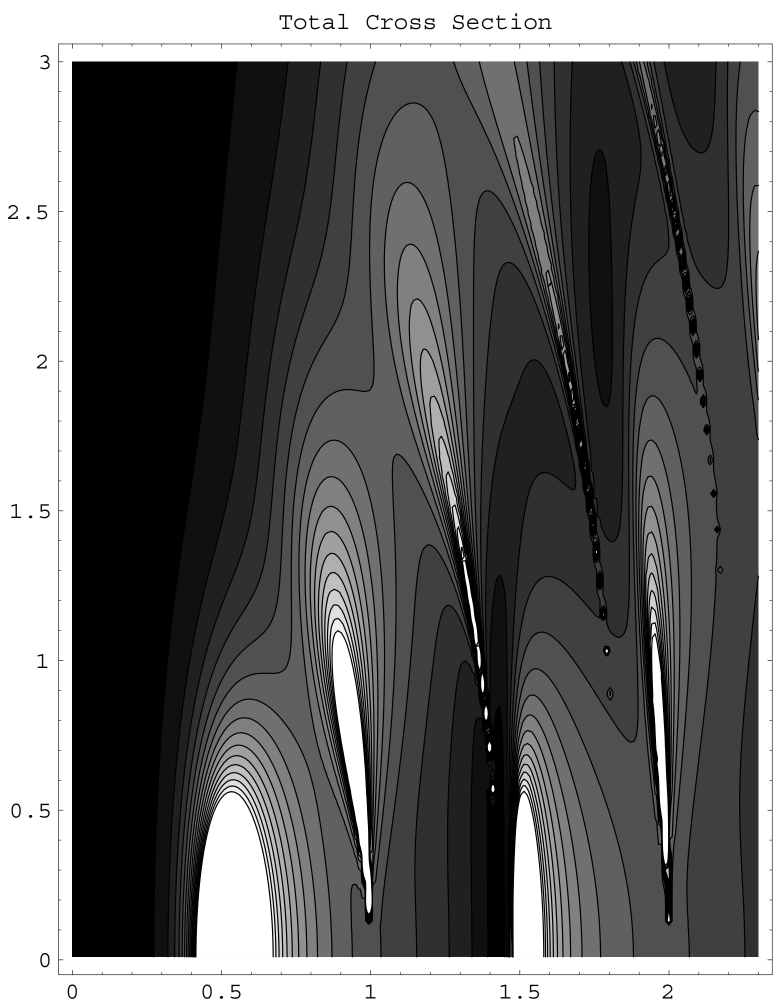

Fig. 5: Total cross section obtained by the summation of the σ_ℓ's

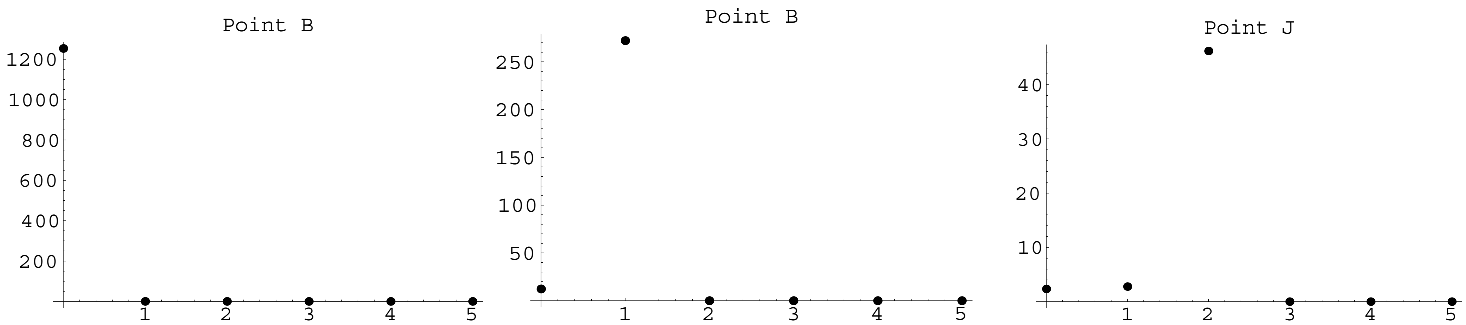

Fig. 6: σ_ℓ vs ℓ for tuples $(0.5\,,0.1)$, $(0.98\,,0.35)$ and $(1.41\,,0.573)$

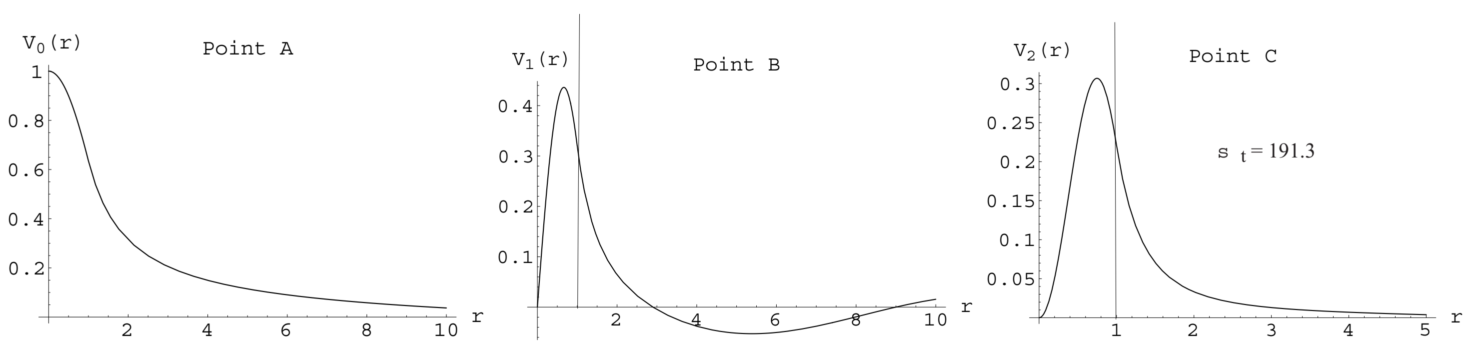

Fig. 7: $v_\ell(r)$ vs r for resonances A, B and C.